Searches for 25 rare and forbidden decays of D^+ and D_s^+ mesons

The LHCb collaboration

E-mail: christopher.burr@cern.ch

ABSTRACT: A search is performed for rare and forbidden charm decays of the form $D_{(s)}^+ \to h^\pm \ell^+ \ell^{(')\mp}$, where $h^\pm$ is a pion or kaon and $\ell^{(')\pm}$ is an electron or muon. The measurements are performed using proton-proton collision data, corresponding to an integrated luminosity of $1.6\,\text{fb}^{-1}$, collected by the LHCb experiment in 2016. No evidence is observed for the 25 decay modes that are investigated and $90\,\%$ confidence level limits on the branching fractions are set between 1.4×10^{-8} and 6.4×10^{-6}. In most cases, these results represent an improvement on existing limits by one to two orders of magnitude.

Contents

1 Introduction

The search for rare and forbidden decays in flavour physics constitutes an important test of the Standard Model (SM) and provides a window to new physics. In the charm sector, decays of the form $D^+ \to h^\pm \ell^+ \ell^{(\prime)\mp}$ and $D_s^+ \to h^\pm \ell^+ \ell^{(\prime)\mp}$, where $h^\pm$ is a charged pion or kaon and $l^{(\prime)\pm}$ is an electron or muon, are among such processes.[1] Searches are reported for 25 decay modes, with common experimental approaches applied to all channels.

The physics processes of these channels vary. Four of the decay channels ($D^+ \to \pi^+ e^+ e^-$, $D^+ \to \pi^+ \mu^+ \mu^-$, $D_s^+ \to K^+ e^+ e^-$, $D_s^+ \to K^+ \mu^+ \mu^-$) involve flavour-changing neutral current (FCNC) transitions. These processes are rare within the Standard Model as only weak annihilation processes can occur at tree level. At the loop level, FCNC transitions are suppressed by the Glashow—Iliopoulos—Maiani (GIM) mechanism [1] but are well established in both B-meson and K-meson decays [2]. FCNC B-meson decays have received significant attention in recent years: the process $B_s^0 \to \mu^+ \mu^-$ was observed [3–6]; and experimental observations in analyses of $b \to s\ell^+\ell^-$ transitions are in tension with the SM predictions (see ref. [7] and references therein). The GIM cancellation in the D-meson system is stronger than in the B-meson system, leading to short-distance SM branching fractions of $\mathcal{O}(10^{-12})$ [8]. These four FCNC decays also proceed through weak annihilation diagrams, as do a further four decays ($D^+ \to K^+ e^+ e^-$, $D^+ \to K^+ \mu^+ \mu^-$, $D_s^+ \to \pi^+ e^+ e^-$, $D_s^+ \to \pi^+ \mu^+ \mu^-$). Significant long-distance contributions occur from dilepton resonances

---

[1]Throughout this article the inclusion of charge-conjugate processes and the use of natural units ($c = \hbar = 1$) is implied, unless otherwise indicated.

and these are expected to dominate the SM contribution across the full dilepton invariant-mass-squared distribution [8, 9].

The eight decay modes with two oppositely charged leptons of different flavour $(D^+_{(s)} \to \pi^+ e^+ \mu^-,\ D^+_{(s)} \to \pi^+ \mu^+ e^-,\ D^+_{(s)} \to K^+ e^+ \mu^-,\ D^+_{(s)} \to K^+ \mu^+ e^-)$ are lepton-flavour violating (LFV) and lepton-number conserving decays. These decays have only negligible contributions from neutrino mixing in the SM. The nine decay modes analysed with same-sign leptons $(D^+_{(s)} \to \pi^- e^+ e^+,\ D^+_{(s)} \to \pi^- \mu^+ \mu^+,\ D^+_s \to K^- e^+ e^+,\ D^+_s \to K^- \mu^+ \mu^+,\ D^+_{(s)} \to \pi^- \mu^+ e^+,\ D^+_s \to K^- \mu^+ e^+)$ are both LFV and lepton-number violating (LNV) decays, and forbidden in the SM. Only the D^+_s variant of $D^+_{(s)} \to K^- \ell^+ \ell^{(\prime)+}$ is studied due to the presence of sizeable background contributions near the D^+ signal peak.

The potential of $c \to u \ell^+ \ell^{\prime -}$ processes to constrain new physics has been discussed in the literature [8–11]. Model-independent constraints on Wilson coefficients in effective field theory have been considered, as have specific classes of models. Recently particular attention has been paid to leptoquark models, due to their potential relevance to the anomalies on $b \to s \ell^+ \ell^-$ processes [12–16].

The analysis reported here is performed on a data sample corresponding to an integrated luminosity of $1.6 \, \text{fb}^{-1}$ collected by the LHCb experiment in 2016. Four resonant decays $(D^+_{(s)} \to (\phi \to \mu^- \mu^+)\ \pi^+,\ D^+_{(s)} \to (\phi \to e^- e^+)\ \pi^+)$ are used for calibration and normalisation. Non-resonant decays with a pion and two same-sign or opposite-sign muons in the final state have previously been searched for by LHCb with no evidence observed [17]. The best limits in the other channels are measured by the BaBar collaboration [18], which has studied all channels, or by the CLEO collaboration, from searches in decay modes with dielectrons in the final state [19].

2   Detector and simulation

The LHCb detector [20, 21] is a single-arm forward spectrometer covering the pseudorapidity range $2 < \eta < 5$, designed for the study of particles containing b or c quarks. The detector includes a high-precision tracking system consisting of a silicon-strip vertex detector surrounding the pp interaction region, a large-area silicon-strip detector located upstream of a dipole magnet with a bending power of about $4 \, \text{Tm}$, and three stations of silicon-strip detectors and straw drift tubes placed downstream of the magnet. The tracking system provides a measurement of the momentum, p, of charged particles with a relative uncertainty that varies from 0.5% at low momentum to 1.0% at $200 \, \text{GeV}$. The minimum distance in the plane transverse to the beam of a track to a primary pp collision vertex (PV), the impact parameter (IP), is measured with a resolution of $(15 + 29/p_{\text{T}}) \, \mu\text{m}$, where p_{T} is the component of the momentum transverse to the beam, in GeV. Different types of charged hadrons are distinguished using information from two ring-imaging Cherenkov detectors. Photons, electrons and hadrons are identified by a calorimeter system consisting of scintillating-pad and preshower detectors, an electromagnetic and a hadronic calorimeter. Muons are identified by a system composed of alternating layers of iron and multiwire proportional chambers.

Simulation is required to model the effects of the detector acceptance and the selection requirements. In the simulation, *pp* collisions are generated using PYTHIA [22, 23] with a specific LHCb configuration [24]. Decays of unstable particles are described by EVTGEN [25], in which final-state radiation is generated using PHOTOS [26]. The interaction of the generated particles with the detector, and its response, are implemented using the GEANT4 toolkit [27, 28] as described in ref. [29].

3 Triggering, reconstruction and selection

The online event selection is performed by a trigger, which consists of a hardware stage, based on information from the calorimeter and muon systems, followed by a two-level software stage. In between the two software stages, an alignment and calibration of the detector is performed in near real time and the results are used in the trigger. The same alignment and calibration information is propagated to the offline reconstruction, ensuring consistent and high-quality particle identification (PID) performance between the trigger and offline software.

A hardware trigger selection is made for all decay channels based on observing a deposit with high transverse energy in the hadronic calorimeter. Depending on the leptons in the final state, this is supplemented by a selection of events with high transverse-energy clusters in the electromagnetic calorimeter and high transverse-momentum muons. At the first software level, inclusive multivariate selections are used to select charged tracks which do not originate from any PV.

The second software level builds $D_{(s)}^+$ candidates using exclusive selections for each combination of final-state particles. Only events containing a single reconstructed PV are used. All three tracks are required to be incompatible with coming from the PV, and to have been reconstructed with good fit quality, have a transverse momentum exceeding 300 MeV and a momentum exceeding 2000 MeV. The tracks are required to form a $D_{(s)}^+$ secondary vertex, with good fit quality and the three dimensional distance between all pairs of tracks to intercept within 150 μm. The angle between the reconstructed $D_{(s)}^+$ and the vector connecting the PV to the decay vertex of the $D_{(s)}^+$ candidate (direction angle) must be within 14 mrad. Loose PID requirements are made on all final-state tracks. Eight of the signal channels in this analysis can proceed via decays through intermediate resonances (η, ρ^0, ω and ϕ). These are removed by vetoing the region [525 MeV, 1250 MeV] in dilepton mass. The resonant channel $D_{(s)}^+ \to (\phi \to \mu^- \mu^+) \, \pi^+ \, (D_{(s)}^+ \to (\phi \to e^- e^+) \, \pi^+)$ is further selected by requiring the invariant mass of the dimuon (dielectron) pair be within $\pm 20 \, (^{+40}_{-100})$ MeV of the ϕ mass [2]. A bremsstrahlung reconstruction procedure is used to correct the momentum of electron candidates.

A classifier trained using XGBoost [30] is used to further distinguish between signal and background originating from random combinations of tracks. A single classifier is trained for each final state, with signal being represented by an equally weighted mixture of simulated D^+ and D_s^+ events. This approach is found to give equivalent performance when compared to using a separate classifier for each signal meson. Background candidates for the training are provided from an identically selected data sample except all three final-

state particles are required to have the same electric charge. The classifier is trained using the fit quality of the primary and secondary vertex, the $D_{(s)}^+$ pseudorapidity, the $D_{(s)}^+$ flight distance, the difference in χ^2 of the PV reconstructed with and without each final-state track, the momentum of each final-state track, the maximum three-dimensional distance of closest approach between all final-state tracks, the direction angle and the reconstructed proper lifetime of the $D_{(s)}^+$. To guarantee that no other tracks can be associated to the secondary vertex, an isolation variable, A_{p_T}, is used that considers the imbalance of p_T of nearby tracks compared to that of the $D_{(s)}^+$ candidate,

$$A_{p_T} = \frac{p_T(D_{(s)}^+) - (\sum \overrightarrow{p})_T}{p_T(D_{(s)}^+) + (\sum \overrightarrow{p})_T}, \tag{3.1}$$

where $p_T(D_{(s)}^+)$ is the p_T of the $D_{(s)}^+$ meson and $(\sum \overrightarrow{p})_T$ is the transverse component of the vector sum of all charged particles momenta within a cone around the candidate, excluding the three signal tracks. The cone is defined by a circle of radius 2.0 in the plane of pseudorapidity and azimuthal angle, measured in radians, around the $D_{(s)}^+$ candidate direction. The signal $D_{(s)}^+$ candidates tend to be more isolated than the combinatorial background and show on average greater values of A_{p_T}. The final selection was optimised using a grid search in the thresholds applied to the classifier output and the PID variables.

4 Invariant-mass distributions

The signal yields are determined using maximum-likelihood fits to the invariant-mass distributions in each of the $D_{(s)}^+ \to h^\pm \ell^+ \ell^{(\prime)\mp}$ final states, including the resonant channels. The fit is performed in the mass range of 1802 to 2050 MeV for all final states where both the D^+ and D_s^+ decay channels are analysed. In the final states where only the D_s^+ contribution is analysed, the fit is performed in the range of 1926 to 2050 MeV. The invariant-mass distributions are shown in figures 1–5, with fits indicated. No evidence is observed in any of the 25 signal channels. The yields obtained from the fit to the normalisation channels can be found in table 1.

The mass distributions for the signal contributions are obtained by modelling the distributions in simulated events with a kernel density estimation (KDE) technique [31]. The same technique is applied to the $D_{(s)}^+ \to (\phi \to e^- e^+) \pi^+$ channels. In the $D_{(s)}^+ \to (\phi \to \mu^- \mu^+) \pi^+$ channels, where a clean separation from background can be made, a fit with a double Gaussian distribution is performed to the data, with the two Gaussian distributions sharing a common mean.

In decay channels with electrons, the observed mass distribution is dependent on the number of reconstructed bremsstrahlung photons. For final states with one electron, separate shapes are extracted from simulation for candidates with no bremsstrahlung and where one or more reconstructed photon candidates are associated with the electron. For final states with two electrons, separate shapes are used for candidates with no bremsstrahlung, one photon per $D_{(s)}^+$ candidate, and two or more photons per $D_{(s)}^+$ candidate.
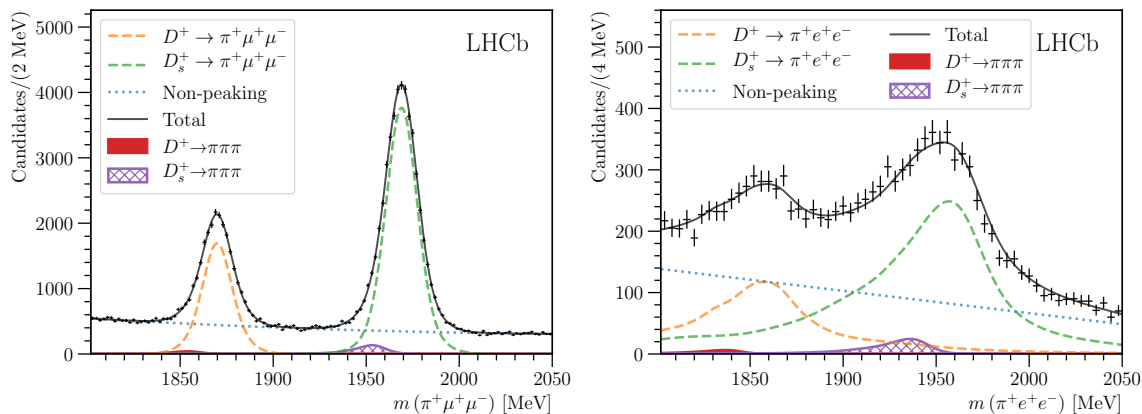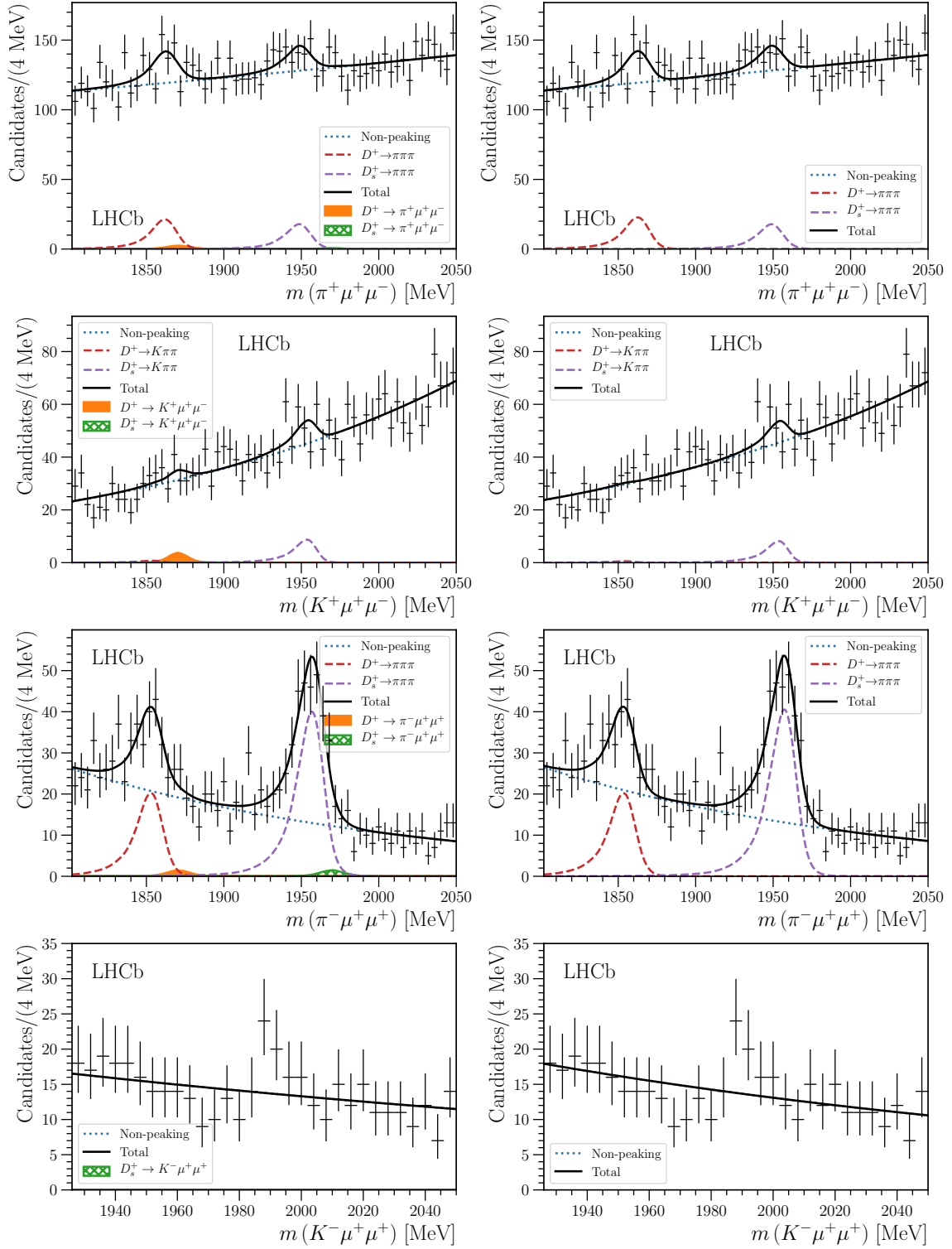
Figure 1. Distributions of the three-body invariant mass for the $D^+_{(s)} \to (\phi \to \ell^- \ell^+)\, \pi^+$ candidates used for normalisation and calibration. The final states are specified in the mass label. The D^+ (D^+_s) signal component is shown as a dashed orange (green) line, peaking backgrounds are denoted by the solid (hashed) regions and the non-peaking background is denoted by the blue dotted line.

Background arises from random combinations which vary smoothly across the fit range, and from misidentified and partially reconstructed backgrounds that may peak in the fitted mass range. The combinatorial backgrounds are fitted with an exponential distribution where the analysed signal channel contains dimuons, while third-order Chebyshev polynomials are used in the cases where the signal channel contains one or two electrons. The function used for modelling these combinatorial backgrounds is determined using a data sample where all three final-state tracks have the same charge and any parameters are left floating in the final fit.

Background from decays involving leptons and neutrinos are found to be negligible for this analysis, with only three-body D^+ and D^+_s hadronic decays contributing to the signal samples. The backgrounds that affect a specific signal channel depend on whether the signal-channel hadron is a pion or a kaon and whether the leptons are of the same or opposite charge. Simulation samples, which do not use a description of the interaction of the particles with the detector material, are generated [32], and are fitted using the same KDE technique as the signal.

The modelling of the backgrounds is validated using data samples where the nominal kinematic selection is applied, but with the particle identification requirements reversed and their values modified from those in the signal selection to enhance the background. The distributions in these enhanced background samples are then fitted with the shapes obtained from the KDE fit to the simplified simulation plus a combinatorial-background description. The four final states of the form $D^+_{(s)} \to K^+ \ell^+ \ell^{(\prime)-}$ have significant contributions from $D^+_{(s)} \to K^+ \pi^+ \pi^-$ decays, and the seven final states of the form $D^+_{(s)} \to \pi^+ \ell^\pm \ell^{(\prime)\mp}$ have significant contributions from $D^+_{(s)} \to \pi^+ \pi^+ \pi^-$ decays. In these cases, the KDE description is smeared by a Gaussian function with mean and width included as free parameters of the fit. After applying the additional smearing a good description is obtained in the background-enhanced samples.
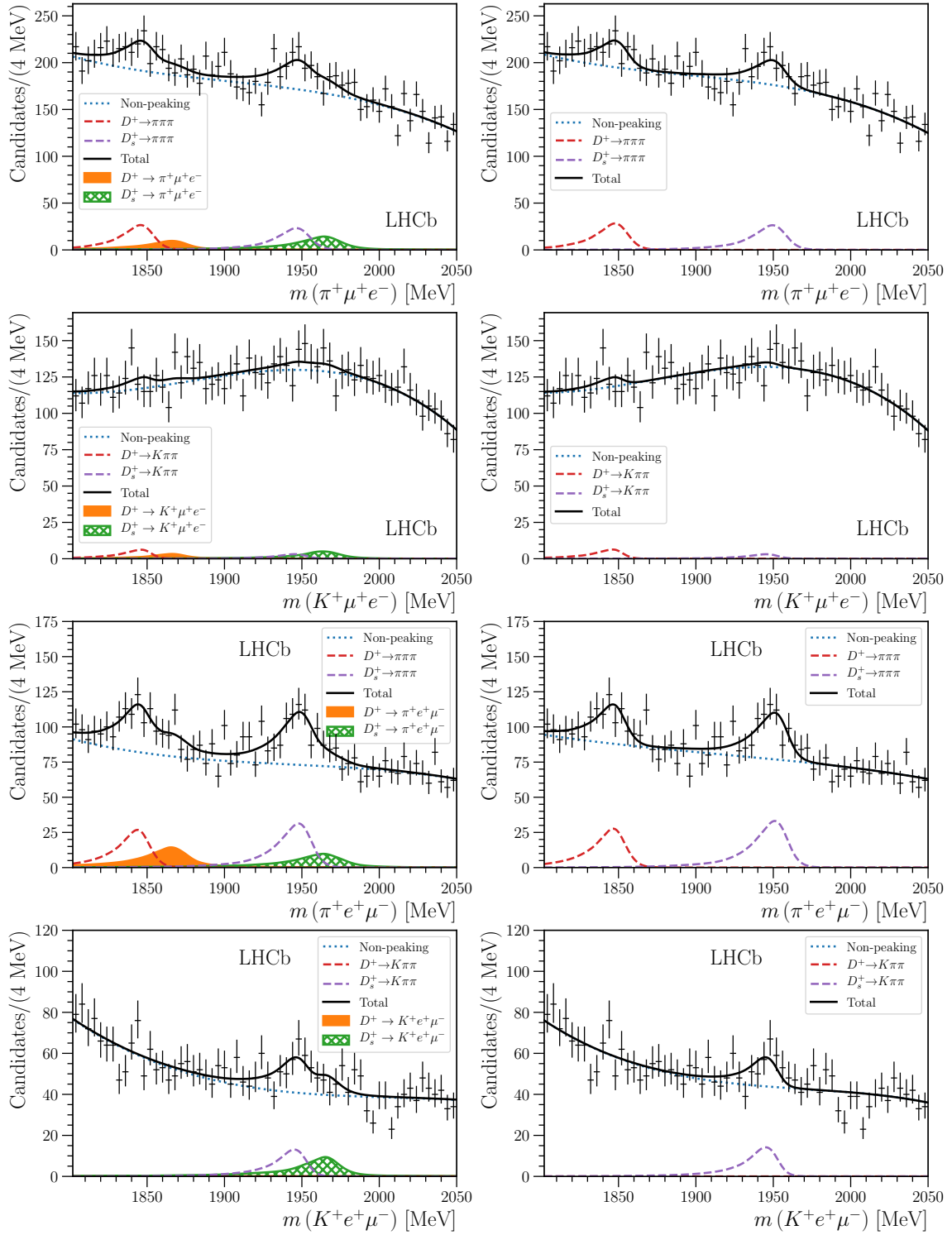
Figure 2. Distributions of the three-body invariant mass in the signal regions for decays with two muons. The final states are specified in the mass label. The left (right) fit with the signal-plus-background (background-only) hypothesis is overlaid with the peaking backgrounds denoted by dashed lines and the non-peaking background is denoted by the blue dotted line.
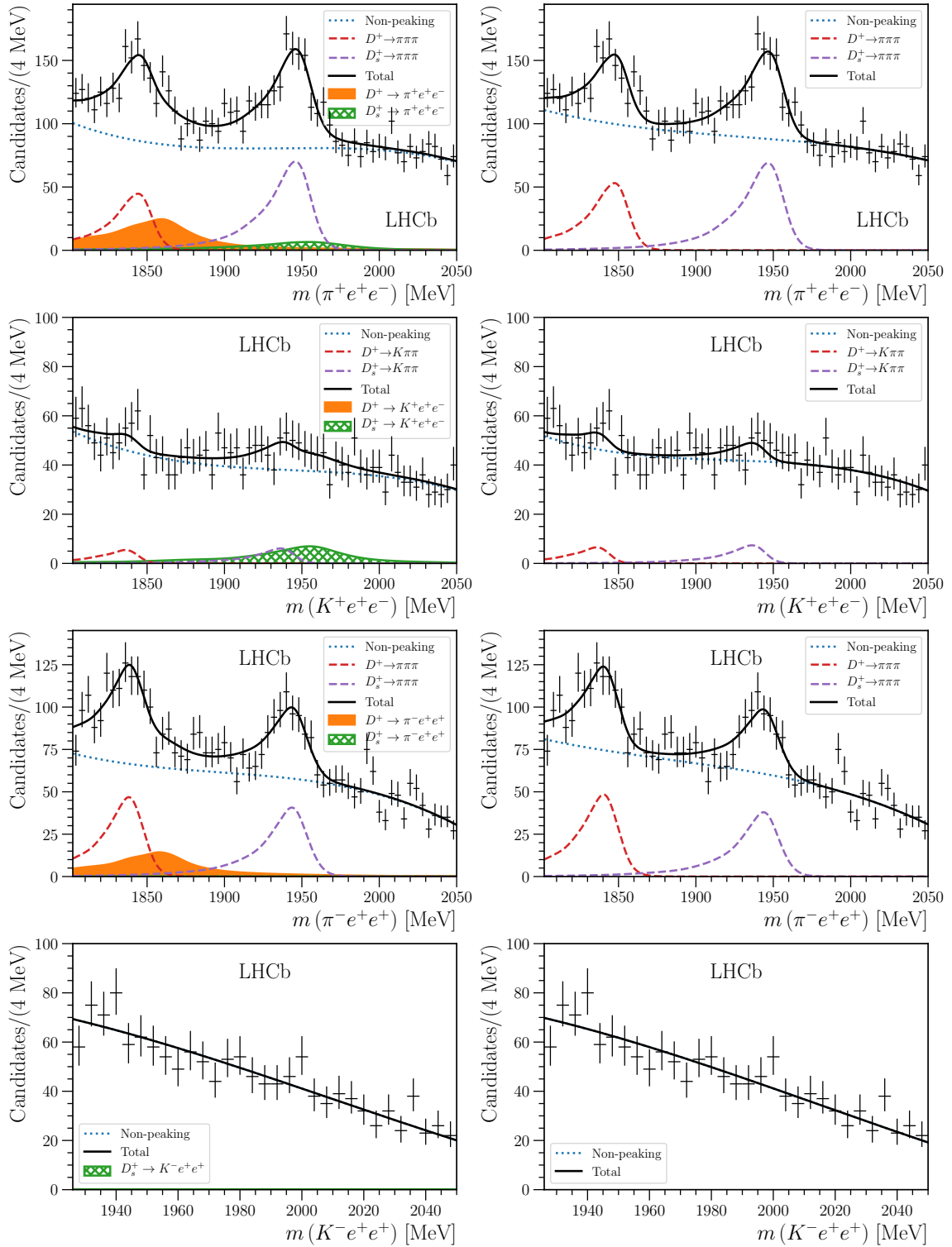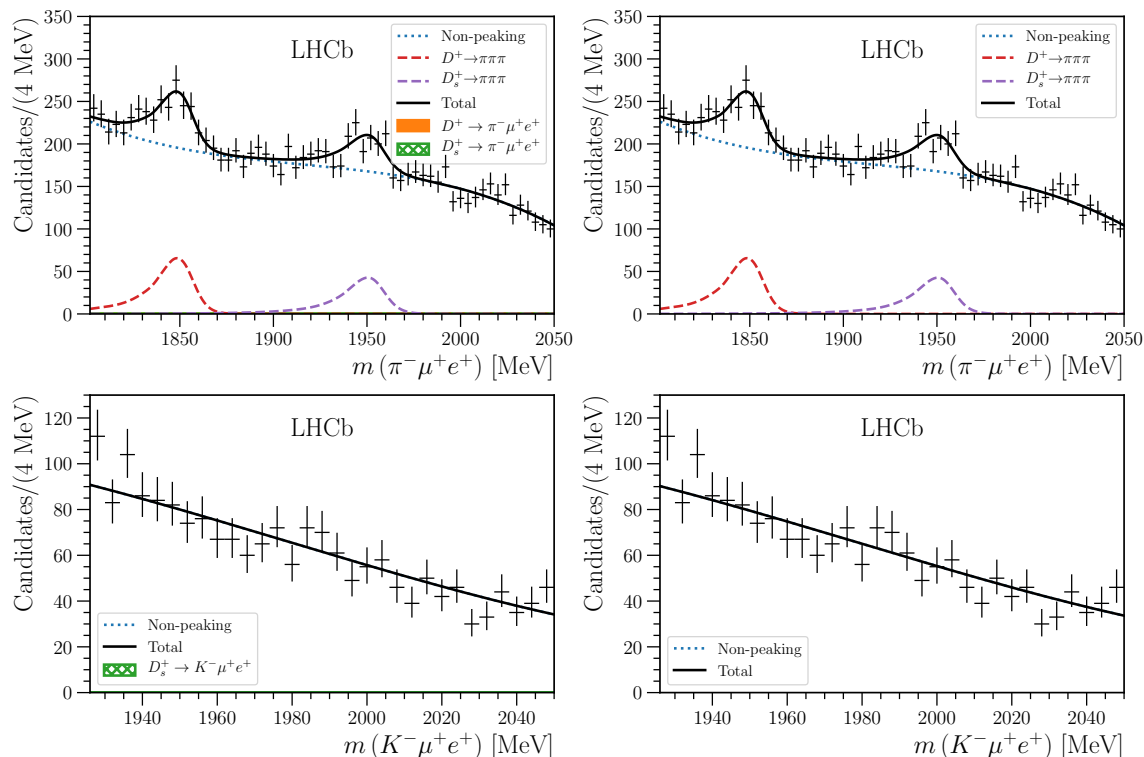
Figure 3. Distributions of the three-body invariant mass in the signal regions for decays with two electrons. The final states are specified in the mass label. The left (right) fit with the signal-plus-background (background-only) hypothesis is overlaid with the peaking backgrounds denoted by dashed lines and the non-peaking background is denoted by the blue dotted line.

Figure 4. Distributions of the three-body invariant mass in the signal regions for decays with an oppositely charged electron and muon. The final states are specified in the mass label. The left (right) fit with the signal-plus-background (background-only) hypothesis is overlaid with the peaking backgrounds denoted by dashed lines and the non-peaking background is denoted by the blue dotted line.

Channel	$\mathcal{B}$ [2]	Fitted yield
$D^+ \to (\phi \to \mu^- \mu^+)\, \pi^+$	$(1.63 \pm 0.12) \times 10^{-6}$	$18\,100 \pm 340$
$D^+ \to (\phi \to e^- e^+)\, \pi^+$	$(1.67 \pm 0.07) \times 10^{-6}$	2160 ± 180
$D_s^+ \to (\phi \to \mu^- \mu^+)\, \pi^+$	$(1.33 \pm 0.10) \times 10^{-5}$	$42\,000 \pm 400$
$D_s^+ \to (\phi \to e^- e^+)\, \pi^+$	$(1.37 \pm 0.05) \times 10^{-5}$	5320 ± 180

Table 1. Reference branching fractions ($\mathcal{B}$) used for the resonant channels alongside signal yields. Here only statistical sources are considered for the fitted yield uncertainties.

Figure 5. Distributions of the three-body invariant mass in the signal regions for decays with an electron and a muon with matching charge. The final states are specified in the mass label. The left (right) fit with the signal-plus-background (background-only) hypothesis is overlaid with the peaking backgrounds denoted by dashed lines and the non-peaking background is denoted by the blue dotted line.

5 Branching fraction determination

The signal branching fractions are obtained from fits to the three-body invariant-mass distributions, shown in figures 2–5. The branching fractions are defined by

$$\mathcal{B}_{D_{(s)}^+ \to h^\pm \ell^+ \ell^{(\prime)\mp}} = \frac{N_{D_{(s)}^+ \to h^\pm \ell^+ \ell^{(\prime)\mp}}}{N_{D_{(s)}^+ \to (\phi \to \mu^+ \mu^-)\pi^+}} \cdot \frac{\epsilon_{D_{(s)}^+ \to (\phi \to \mu^+ \mu^-)\pi^+}}{\epsilon_{D_{(s)}^+ \to h^\pm \ell^+ \ell^{(\prime)\mp}}} \cdot \mathcal{B}_{D_{(s)}^+ \to (\phi \to \mu^+ \mu^-)\pi^+} \tag{5.1}$$

where N is the fitted yield in the channel indicated, $\mathcal{B}$ is the branching fraction and ϵ is the efficiency of the selection criteria. The branching fraction used for $D_{(s)}^+ \to (\phi \to \ell^- \ell^+)\, \pi^+$ can be found in table 1 and is obtained by combining the measurements of $D_{(s)}^+ \to (\phi \to K^+ K^-)\, \pi^+$, $\phi \to K^+ K^-$ and $\phi \to \ell^+ \ell^-$ from ref. [2]. The systematic uncertainties are described in section 6 and taken into account with a log-normal distribution in the branching fraction fit. The potential overlap between the D^+ and D_s^+ signal peaks in the same final state is accounted for by floating the yield of the other meson in each fit and treating this as an additional nuisance parameter when computing the significance of the signal peak.

Data and simulation are found to be within good agreeement and the quality of the modelling for the three-body invariant mass can be seen in figure 1. The effect of discrepancies between data and simulation are further reduced by using a reweighting technique that utilises a multivariate classifier. This classifier is used to generate per-event weights using the method outlined in ref. [33]. The procedure is applied separately for each of the calibration channels and each classifier is trained to distinguish between real and simulated calibration-channel events. Background subtraction of the data is applied using the *sPlot* technique [34] with a fit to the invariant mass of the calibration channel. The weights obtained from these classifiers are applied to the simulation and then used throughout this analysis. Decay channels with two electrons in the final state use weights from the $D_{(s)}^+ \to (\phi \to e^- e^+)\, \pi^+$ classifiers and all other decays use the $D_{(s)}^+ \to (\phi \to \mu^- \mu^+)\, \pi^+$ classifiers. In all cases the same parent particle $(D_{(s)}^+)$ decay as the signal is used.

Equation (5.1) includes the ratio of efficiencies between the normalisation channel and the signal channel so that the effects of several systematic uncertainties cancel. The reconstruction and selection efficiencies are obtained from simulation with the aforementioned corrections applied. As the resonant structure in the signal channels is inherently unknown, the efficiency of each signal decay is obtained under the assumption that the decay particles are uniformly distributed across the phase space with the signal contribution extrapolated into any vetoed kinematic regions.

The efficiency with which events pass the PID requirements is obtained using a set of calibration channels. The PID response is sampled [35] as a function of the particle kinematics and event multiplicity in simulation, as described in ref. [36]. A small correction is made for differences in the track reconstruction efficiency between data and simulation [37].

For channels containing electrons, an additional correction is applied to the ratio of electron to muon reconstruction efficiencies. This is computed under the assumption that the correction for each electron is independent of the other, and thus the square root of the efficiency-corrected signal-yield ratio between the calibration channels $D_{(s)}^+ \to (\phi \to e^- e^+)\, \pi^+$ and $D_{(s)}^+ \to (\phi \to \mu^- \mu^+)\, \pi^+$ in data is taken.

The single event sensitivities, i.e. the branching fractions corresponding to a single observed signal event, vary from 3×10^{-10} to 1×10^{-8} depending on the channel. To ensure the efficiencies are sufficiently well understood, cross-check measurements are made of the branching fractions of $D_{(s)}^+ \to (\phi \to \mu^- \mu^+)\, \pi^+$ and $D_{(s)}^+ \to (\phi \to e^- e^+)\, \pi^+$ decays. The results obtained before and after applying the offline selection criteria are compared and found to be in agreement.

6 Systematic uncertainties

The efficiency ratio in eq. (5.1) is affected by several sources of systematic uncertainty. The finite size of the simulated signal event samples introduces a systematic uncertainty on the branching fractions varying from 1.4 % to 6.4 %. A summary of the systematic uncertainties assigned for each effect is given in table 2.

The track-reconstruction efficiency from simulation is corrected using a tag-and-probe technique in data where $J/\psi \to \mu^+\mu^-$ decays are selected by making requirements on only one muon. This is found to have negligible effect on the efficiency ratio. A 0.8 % systematic uncertainty is assigned for each particle species in the signal decay that differs from that of the $D^+_{(s)} \to (\phi \to \mu^-\mu^+) \pi^+$ reference. An additional 1.5 % systematic uncertainty is assigned to channels containing a kaon to account for possible hadronic interaction effects with the detector material [37]. Alternative parametrisations [36] are considered for the sampling of the PID response, but their associated systematic effects have negligible impact compared to the statistical uncertainties of the analysis and other sources of systematic uncertainty. For final states with both a muon and an electron, a further systematic uncertainty of 7.6 % is assigned for the choice of reweighting classifier. This is obtained from the RMS of the change in efficiency of all mixed-lepton final states, using the alternative reweighting classifier.

The systematic uncertainties affecting the signal yield are estimated using an alternative fit model for the normalisation channels. For signal states with two muons, a KDE parametrisation obtained from simulation is used as an alternative for the nominal model describing the $D^+_{(s)} \to (\phi \to \mu^-\mu^+) \pi^+$ signal. In all other cases, the differences are most likely to arise from the treatment of bremsstrahlung radiation in simulation. Therefore, an alternative model is generated by fixing the relative yield between the three bremsstrahlung categories of $D^+_{(s)} \to (\phi \to e^-e^+) \pi^+$ from simulation. The signal yield from the alternative models is compared with the nominal model and the difference is assigned as a systematic uncertainty.

The uncertainty on the yield of $D^+_{(s)} \to (\phi \to \mu^-\mu^+) \pi^+$ is dominated by the modelling of the $D^+_{(s)} \to \pi^+\pi^+\pi^-$ backgrounds in the lower tails of the larger signal components. To account for this, the data set is refitted neglecting these background components, and the change in signal yield is assigned as a systematic uncertainty. The same procedure is applied for $D^+_{(s)} \to (\phi \to e^-e^+) \pi^+$ with the change in signal yield used as the uncertainty on the electron efficiency correction factor.

7 Results and conclusions

No significant deviation from the background only hypothesis is found for any of the channels and all limits are within $\pm 2\sigma$ of the expected limit. The compatibility of the observed mass-distributions with a signal-plus-background or a background-only hypothesis is evaluated using the CL_s method as described in refs. [38, 39] with systematic uncertainties included with log-normal uncertainties. Upper limits on the branching fractions are determined using the observed distribution of CL_s as a function of the assumed branching

Channel	Simulated signal sample [%]	Track-reconstruction efficiency [%]	Reweighting [%]	Signal [%]	$\phi \to \mu^-\mu^+$ yield [%]	$\phi \to e^-e^+$ $\epsilon_{\text{electron}}$ [%]
$D^+ \to K^+e^+e^-$	6.4	3.2	–	7.0	2.0	9.1
$D^+ \to K^+e^+\mu^-$	2.1	2.5	7.6	7.0	2.0	4.6
$D^+ \to K^+\mu^+e^-$	1.8	2.5	7.6	7.0	2.0	4.6
$D^+ \to K^+\mu^+\mu^-$	3.0	2.3	–	0.8	2.0	–
$D^+ \to \pi^+e^+e^-$	3.9	2.3	–	7.0	2.0	9.1
$D^+ \to \pi^-e^+e^+$	2.6	2.3	–	7.0	2.0	9.1
$D^+ \to \pi^+e^+\mu^-$	1.9	1.1	7.6	7.0	2.0	4.6
$D^+ \to \pi^+\mu^+e^-$	1.5	1.1	7.6	7.0	2.0	4.6
$D^+ \to \pi^-\mu^+e^+$	1.6	1.1	7.6	7.0	2.0	4.6
$D^+ \to \pi^+\mu^+\mu^-$	1.9	0.1	–	0.8	2.0	–
$D^+ \to \pi^-\mu^+\mu^+$	1.5	0.0	–	0.8	2.0	–
$D_s^+ \to K^+e^+e^-$	6.0	3.2	–	7.0	3.0	7.5
$D_s^- \to K^-e^+e^+$	3.2	3.2	–	7.0	3.0	7.5
$D_s^+ \to K^+e^+\mu^-$	3.0	2.5	7.6	7.0	3.0	3.8
$D_s^+ \to K^+\mu^+e^-$	2.5	2.5	7.6	7.0	3.0	3.8
$D_s^+ \to K^-\mu^+e^+$	2.4	2.5	7.6	7.0	3.0	3.8
$D_s^+ \to K^+\mu^+\mu^-$	3.3	2.3	–	0.8	3.0	–
$D_s^+ \to K^-\mu^+\mu^+$	1.8	2.3	–	0.8	3.0	–
$D_s^+ \to \pi^+e^+e^-$	4.3	2.3	–	7.0	3.0	7.5
$D_s^+ \to \pi^-e^+e^+$	3.1	2.3	–	7.0	3.0	7.5
$D_s^+ \to \pi^+e^+\mu^-$	2.7	1.2	7.6	7.0	3.0	3.8
$D_s^+ \to \pi^+\mu^+e^-$	2.3	1.1	7.6	7.0	3.0	3.8
$D_s^+ \to \pi^-\mu^+e^+$	2.2	1.2	7.6	7.0	3.0	3.8
$D_s^+ \to \pi^+\mu^+\mu^-$	2.5	0.1	–	0.8	3.0	–
$D_s^+ \to \pi^-\mu^+\mu^+$	2.2	0.0	–	0.8	3.0	–

Table 2. Summary of systematic uncertainties for each signal decay. The "$\phi \to \mu^-\mu^+$ yield" column represents the combination of the statistical uncertainty from the $D_{(s)}^+ \to (\phi \to \mu^-\mu^+)\,\pi^+$ dataset with the systematic uncertainty from the modelling of the $D_{(s)}^+ \to \pi^+\pi^+\pi^-$ backgrounds. A further 7.6 % uncertainty from the branching fraction of $D_{(s)}^+ \to (\phi \to \mu^-\mu^+)\,\pi^+$ and a 1.0 % uncertainty from the finite size of the simulated $D_{(s)}^+ \to (\phi \to \mu^-\mu^+)\,\pi^+$ sample apply to all channels. The electron efficiency correction, described at the end of section 5, is denoted by $\epsilon_{\text{electron}}$. All values are given in percent as a fractional uncertainty on the signal yield.

| Decay | Branching fraction upper limit [10^{-9}] | | | | | |
| | D^+ | | | D_s^+ | | |
	SES	90 % CL	95 % CL	SES	90 % CL	95 % CL
$D_{(s)}^+ \to \pi^+ \mu^+ \mu^-$	0.6	67	74	2.4	180	210
$D_{(s)}^+ \to \pi^- \mu^+ \mu^+$	0.3	14	16	1.8	86	96
$D_{(s)}^+ \to K^+ \mu^+ \mu^-$	1.2	54	61	3.8	140	160
$D_{(s)}^+ \to K^- \mu^+ \mu^+$	-	-	-	1.2	26	30
$D_{(s)}^+ \to \pi^+ e^+ \mu^-$	0.6	210	230	3.1	1100	1200
$D_{(s)}^+ \to \pi^+ \mu^+ e^-$	0.4	220	220	2.2	940	1100
$D_{(s)}^+ \to \pi^- \mu^+ e^+$	0.4	130	150	2.0	630	710
$D_{(s)}^+ \to K^+ e^+ \mu^-$	0.7	75	83	3.7	790	880
$D_{(s)}^+ \to K^+ \mu^+ e^-$	0.5	100	110	2.5	560	640
$D_{(s)}^+ \to K^- \mu^+ e^+$	-	-	-	2.4	260	320
$D_{(s)}^+ \to \pi^+ e^+ e^-$	1.9	1600	1800	8.1	5500	6400
$D_{(s)}^+ \to \pi^- e^+ e^+$	0.9	530	600	4.1	1400	1600
$D_{(s)}^+ \to K^+ e^+ e^-$	4.4	850	1000	14.8	4900	5500
$D_{(s)}^+ \to K^- e^+ e^+$	-	-	-	4.1	770	840

Table 3. The single event sensitivities (SES), and upper limits on the branching fractions obtained using the CL$_s$ method, for each signal decay channel.

fraction. The upper limits at 90 % and 95 % confidence level (CL) are given in table 3 and are shown in figure 6.

In conclusion, searches have been made for 25 previously unobserved three-body decays of D^+ and D_s^+ mesons using $1.6\,\mathrm{fb}^{-1}$ of pp collision data collected by the LHCb experiment during 2016. The decays are of the form $D_{(s)}^+ \to h^\pm \ell^+ \ell^{(\prime)\mp}$ where h is a kaon or pion and $\ell^{(\prime)}$ is an electron or muon and the results are computed under the assumption that the decay particles are uniformly distributed across the phase space. No significant deviations from the background-only hypotheses are seen. The 90 % CL limits on the branching fractions vary from 1.4×10^{-8} to 6.4×10^{-6} and represent the world's best limits for 23 of these decays. In the majority of the channels the improvement on previous limits is more than an order of magnitude, with the largest improvement being a factor of five hundred in $D_s^+ \to K^- \mu^+ \mu^+$ decays.
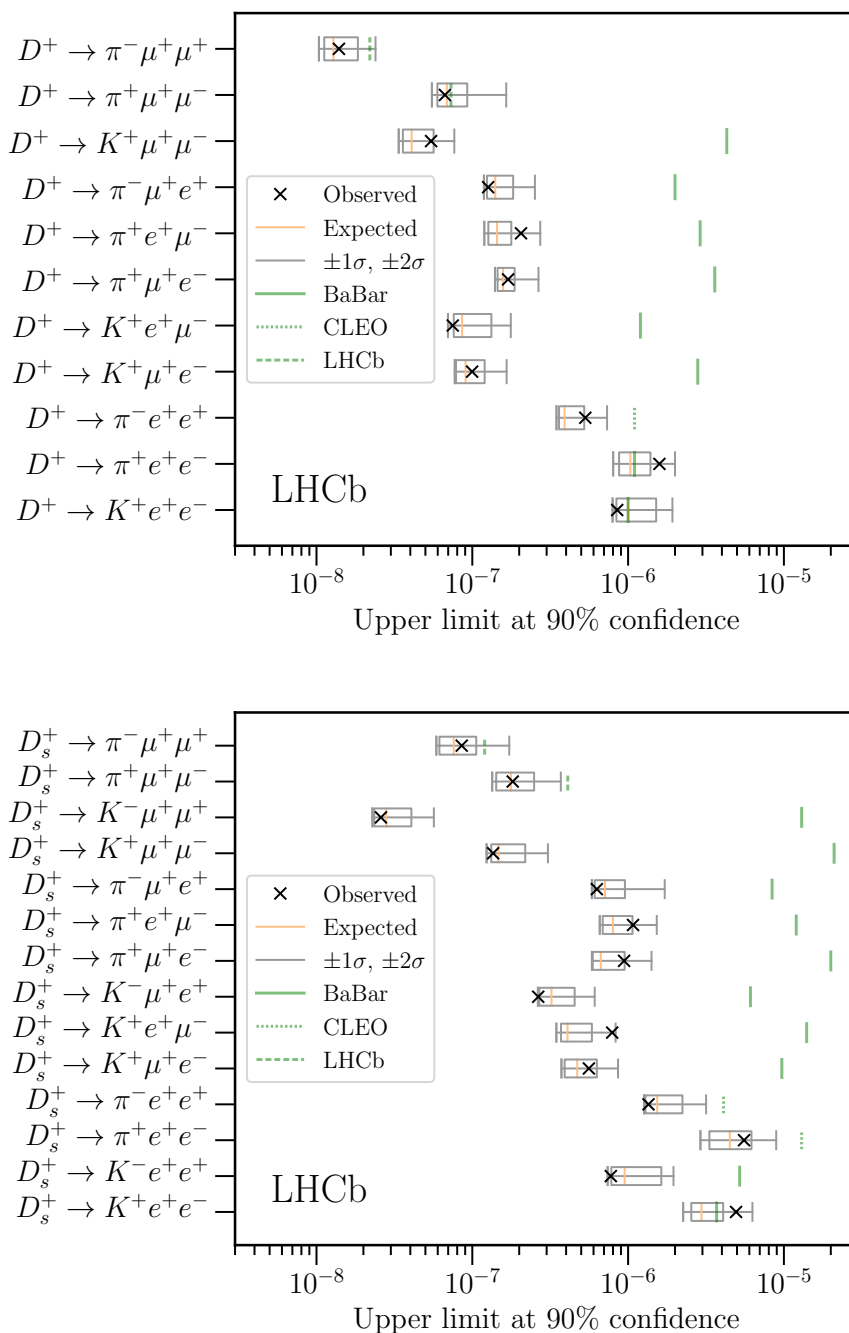
Figure 6. Upper limits at 90 % confidence level on the $D^+_{(s)}$ signal channels. The median (orange), $\pm 1\sigma$ and $\pm 2\sigma$ expected limits are shown as box plots and the observed limit is given by a black cross. The green line shows the previous world's best limit for each channel where the solid, dotted and dashed lines correspond to BaBar, CLEO and LHCb [17–19]. The expected limits are determined using pseudo-experiments to approximate the CL$_s$ distribution under the background-only hypothosis.

Acknowledgments

References

[1] S.L. Glashow, J. Iliopoulos and L. Maiani, *Weak interactions with lepton-hadron symmetry*, *Phys. Rev. D* **2** (1970) 1285 [INSPIRE].

[2] PARTICLE DATA GROUP collaboration, *Review of particle physics*, *Phys. Rev. D* **98** (2018) 030001 [INSPIRE] [http://pdg.lbl.gov].

[3] CMS and LHCb collaborations, *Observation of the rare $B_s^0 \to \mu^+\mu^-$ decay from the combined analysis of CMS and LHCb data*, *Nature* **522** (2015) 68 [arXiv:1411.4413] [INSPIRE].

[4] LHCb collaboration, *Measurement of the $B_s^0 \to \mu^+\mu^-$ branching fraction and effective lifetime and search for $B^0 \to \mu^+\mu^-$ decays*, *Phys. Rev. Lett.* **118** (2017) 191801 [arXiv:1703.05747] [INSPIRE].

[5] CMS collaboration, *Measurement of properties of $B_s^0 \to \mu^+\mu^-$ decays and search for $B^0 \to \mu^+\mu^-$ with the CMS experiment*, *JHEP* **04** (2020) 188 [arXiv:1910.12127] [INSPIRE].

[6] ATLAS collaboration, *Study of the rare decays of B_s^0 and B^0 mesons into muon pairs using data collected during 2015 and 2016 with the ATLAS detector*, *JHEP* **04** (2019) 098 [arXiv:1812.03017] [INSPIRE].

[7] LHCb collaboration, *Search for lepton-universality violation in $B^+ \to K^+\ell^+\ell^-$ decays*, *Phys. Rev. Lett.* **122** (2019) 191801 [`arXiv:1903.09252`] [ɪɴSPIRE].

[8] S. de Boer and G. Hiller, *Flavor and new physics opportunities with rare charm decays into leptons*, *Phys. Rev. D* **93** (2016) 074001 [`arXiv:1510.00311`] [ɪɴSPIRE].

[9] S. Fajfer and N. Košnik, *Prospects of discovering new physics in rare charm decays*, *Eur. Phys. J. C* **75** (2015) 567 [`arXiv:1510.00965`] [ɪɴSPIRE].

[10] R. Bause, M. Golz, G. Hiller and A. Tayduganov, *The new physics reach of null tests with $D \to \pi\ell\ell$ and $D_s \to K\ell\ell$ decays*, *Eur. Phys. J. C* **80** (2020) 65 [*Erratum ibid.* **81** (2021) 219] [`arXiv:1909.11108`] [ɪɴSPIRE].

[11] R. Bause, H. Gisbert, M. Golz and G. Hiller, *Exploiting CP-asymmetries in rare charm decays*, *Phys. Rev. D* **101** (2020) 115006 [`arXiv:2004.01206`] [ɪɴSPIRE].

[12] A. Paul, I.I. Bigi and S. Recksiegel, *On $D \to X_u l^+ l^-$ within the standard model and frameworks like the littlest Higgs model with T parity*, *Phys. Rev. D* **83** (2011) 114006 [`arXiv:1101.6053`] [ɪɴSPIRE].

[13] G. Burdman, E. Golowich, J.L. Hewett and S. Pakvasa, *Rare charm decays in the standard model and beyond*, *Phys. Rev. D* **66** (2002) 014009 [`hep-ph/0112235`] [ɪɴSPIRE].

[14] R.-M. Wang, J.-H. Sheng, J. Zhu, Y.-Y. Fan and Y. Gao, *Studying the lepton number and lepton flavor violating $D0 \to e^\pm\mu^\mp$ and $D_{d/s}^+ \to \pi(K)^+ e^\pm\mu^\mp$ decays*, *Int. J. Mod. Phys. A* **29** (2014) 1450169 [ɪɴSPIRE].

[15] C. Delaunay, J.F. Kamenik, G. Perez and L. Randall, *Charming CP-violation and Dipole Operators from RS Flavor Anarchy*, *JHEP* **01** (2013) 027 [`arXiv:1207.0474`] [ɪɴSPIRE].

[16] A. Paul, A. De La Puente and I.I. Bigi, *Manifestations of warped extra dimension in rare charm decays and asymmetries*, *Phys. Rev. D* **90** (2014) 014035 [`arXiv:1212.4849`] [ɪɴSPIRE].

[17] LHCb collaboration, *Search for $D_{(s)}^+ \to \pi^+\mu^+\mu^-$ and $D_{(s)}^+ \to \pi^-\mu^+\mu^+$ decays*, *Phys. Lett. B* **724** (2013) 203 [`arXiv:1304.6365`] [ɪɴSPIRE].

[18] BaBar collaboration, *Searches for rare or forbidden semileptonic charm decays*, *Phys. Rev. D* **84** (2011) 072006 [`arXiv:1107.4465`] [ɪɴSPIRE].

[19] CLEO collaboration, *Search for rare and forbidden decays of charm and charmed-strange mesons to final states $h^\pm e^\mp e^+$*, *Phys. Rev. D* **82** (2010) 092007 [`arXiv:1009.1606`] [ɪɴSPIRE].

[20] LHCb collaboration, *The LHCb detector at the LHC*, 2008 *JINST* **3** S08005 [ɪɴSPIRE].

[21] LHCb collaboration, *LHCb detector performance*, *Int. J. Mod. Phys. A* **30** (2015) 1530022 [`arXiv:1412.6352`] [ɪɴSPIRE].

[22] T. Sjöstrand, S. Mrenna and P.Z. Skands, *A brief introduction to PYTHIA 8.1*, *Comput. Phys. Commun.* **178** (2008) 852 [`arXiv:0710.3820`] [ɪɴSPIRE].

[23] T. Sjöstrand, S. Mrenna and P.Z. Skands, *PYTHIA 6.4 physics and manual*, *JHEP* **05** (2006) 026 [`hep-ph/0603175`] [ɪɴSPIRE].

[24] LHCb collaboration, *Handling of the generation of primary events in Gauss, the LHCb simulation framework*, *J. Phys. Conf. Ser.* **331** (2011) 032047 [ɪɴSPIRE].

[25] D.J. Lange, *The EvtGen particle decay simulation package*, *Nucl. Instrum. Meth. A* **462** (2001) 152 [ɪɴSPIRE].

[26] P. Golonka and Z. Was, *PHOTOS Monte Carlo: A Precision tool for QED corrections in Z and W decays*, *Eur. Phys. J. C* **45** (2006) 97 [hep-ph/0506026] [INSPIRE].

[27] GEANT4 collaboration, *Geant4 developments and applications*, *IEEE Trans. Nucl. Sci.* **53** (2006) 270.

[28] GEANT4 collaboration, *Geant4: A simulation toolkit*, *Nucl. Instrum. Meth. A* **506** (2003) 250 [INSPIRE].

[29] LHCb collaboration, *The LHCb simulation application, Gauss: Design, evolution and experience*, *J. Phys. Conf. Ser.* **331** (2011) 032023 [INSPIRE].

[30] T. Chen and C. Guestrin, *XGBoost: A Scalable Tree Boosting System*, in *Proceedings of the 22nd ACM SIGKDD International Conference on Knowledge Discovery and Data Mining*, KDD '16, New York, U.S.A. (2016) arXiv:1603.02754 [INSPIRE].

[31] K.S. Cranmer, *Kernel estimation in high-energy physics*, *Comput. Phys. Commun.* **136** (2001) 198 [hep-ex/0011057] [INSPIRE].

[32] G.A. Cowan, D.C. Craik and M.D. Needham, *RapidSim: an application for the fast simulation of heavy-quark hadron decays*, *Comput. Phys. Commun.* **214** (2017) 239 [arXiv:1612.07489] [INSPIRE].

[33] A. Rogozhnikov, *Reweighting with boosted decision trees*, *J. Phys. Conf. Ser.* **762** (2016) 012036 [arXiv:1608.05806] [INSPIRE].

[34] M. Pivk and F.R. Le Diberder, *sPlot: A statistical tool to unfold data distributions*, *Nucl. Instrum. Meth. A* **555** (2005) 356 [physics/0402083] [INSPIRE].

[35] A. Poluektov, *Kernel density estimation of a multidimensional efficiency profile*, 2015 *JINST* **10** P02011 [arXiv:1411.5528] [INSPIRE].

[36] R. Aaij et al., *Selection and processing of calibration samples to measure the particle identification performance of the LHCb experiment in Run 2*, *EPJ Tech. Instrum.* **6** (2019) 1 [arXiv:1803.00824] [INSPIRE].

[37] LHCb collaboration, *Measurement of the track reconstruction efficiency at LHCb*, 2015 *JINST* **10** P02007 [arXiv:1408.1251] [INSPIRE].

[38] A.L. Read, *Presentation of search results: The CL_s technique*, *J. Phys. G* **28** (2002) 2693 [INSPIRE].

[39] T. Junk, *Confidence level computation for combining searches with small statistics*, *Nucl. Instrum. Meth. A* **434** (1999) 435 [hep-ex/9902006] [INSPIRE].

The LHCb collaboration

R. Aaij[31], C. Abellán Beteta[49], T. Ackernley[59], B. Adeva[45], M. Adinolfi[53], H. Afsharnia[9],
C.A. Aidala[83], S. Aiola[25], Z. Ajaltouni[9], S. Akar[64], J. Albrecht[14], F. Alessio[47], M. Alexander[58],
A. Alfonso Albero[44], Z. Aliouche[61], G. Alkhazov[37], P. Alvarez Cartelle[47], A.A. Alves Jr[45],
S. Amato[2], Y. Amhis[11], L. An[21], L. Anderlini[21], G. Andreassi[48], A. Andreianov[37],
M. Andreotti[20], F. Archilli[16], A. Artamonov[43], M. Artuso[67], K. Arzymatov[41], E. Aslanides[10],
M. Atzeni[49], B. Audurier[11], S. Bachmann[16], M. Bachmayer[48], J.J. Back[55], S. Baker[60],
P. Baladron Rodriguez[45], V. Balagura[11,b], W. Baldini[20], J. Baptista Leite[1], R.J. Barlow[61],
S. Barsuk[11], W. Barter[60], M. Bartolini[23,47,i], F. Baryshnikov[80], J.M. Basels[13], G. Bassi[28],
V. Batozskaya[35], B. Batsukh[67], A. Battig[14], A. Bay[48], M. Becker[14], F. Bedeschi[28], I. Bediaga[1],
A. Beiter[67], V. Belavin[41], S. Belin[26], V. Bellee[48], K. Belous[43], I. Belov[39], I. Belyaev[38],
G. Bencivenni[22], E. Ben-Haim[12], S. Benson[31], A. Berezhnoy[39], R. Bernet[49], D. Berninghoff[16],
H.C. Bernstein[67], C. Bertella[47], E. Bertholet[12], A. Bertolin[27], C. Betancourt[49], F. Betti[19,e],
M.O. Bettler[54], Ia. Bezshyiko[49], S. Bhasin[53], J. Bhom[33], L. Bian[72], M.S. Bieker[14], S. Bifani[52],
P. Billoir[12], M. Birch[60], F.C.R. Bishop[54], A. Bizzeti[21,u], M. Bjørn[62], M.P. Blago[47], T. Blake[55],
F. Blanc[48], S. Blusk[67], D. Bobulska[58], V. Bocci[30], J.A. Boelhauve[14], O. Boente Garcia[45],
T. Boettcher[63], A. Boldyrev[81], A. Bondar[42,x], N. Bondar[37,47], S. Borghi[61], M. Borisyak[41],
M. Borsato[16], J.T. Borsuk[33], S.A. Bouchiba[48], T.J.V. Bowcock[59], A. Boyer[47], C. Bozzi[20],
M.J. Bradley[60], S. Braun[65], A. Brea Rodriguez[45], M. Brodski[47], J. Brodzicka[33],
A. Brossa Gonzalo[55], D. Brundu[26], E. Buchanan[53], A. Büchler-Germann[49], A. Buonaura[49],
C. Burr[47], A. Bursche[26], A. Butkevich[40], J.S. Butter[31], J. Buytaert[47], W. Byczynski[47],
S. Cadeddu[26], H. Cai[72], R. Calabrese[20,g], L. Calefice[14], L. Calero Diaz[22], S. Cali[22],
R. Calladine[52], M. Calvi[24,j], M. Calvo Gomez[44,m], P. Camargo Magalhaes[53], A. Camboni[44],
P. Campana[22], D.H. Campora Perez[47], A.F. Campoverde Quezada[5], S. Capelli[24,j],
L. Capriotti[19,e], A. Carbone[19,e], G. Carboni[29], R. Cardinale[23,i], A. Cardini[26], I. Carli[6],
P. Carniti[24,j], K. Carvalho Akiba[31], A. Casais Vidal[45], G. Casse[59], M. Cattaneo[47],
G. Cavallero[47], S. Celani[48], R. Cenci[28], J. Cerasoli[10], A.J. Chadwick[59], M.G. Chapman[53],
M. Charles[12], Ph. Charpentier[47], G. Chatzikonstantinidis[52], C.A. Chavez Barajas[59],
M. Chefdeville[8], V. Chekalina[41], C. Chen[3], S. Chen[26], A. Chernov[33], S.-G. Chitic[47],
V. Chobanova[45], S. Cholak[48], M. Chrzaszcz[33], A. Chubykin[37], V. Chulikov[37], P. Ciambrone[22],
M.F. Cicala[55], X. Cid Vidal[45], G. Ciezarek[47], P.E.L. Clarke[57], M. Clemencic[47], H.V. Cliff[54],
J. Closier[47], J.L. Cobbledick[61], V. Coco[47], J.A.B. Coelho[11], J. Cogan[10], E. Cogneras[9],
L. Cojocariu[36], P. Collins[47], T. Colombo[47], L. Congedo[18], A. Contu[26], N. Cooke[52], G. Coombs[58],
S. Coquereau[44], G. Corti[47], C.M. Costa Sobral[55], B. Couturier[47], D.C. Craik[63], J. Crkovská[66],
M. Cruz Torres[1,z], R. Currie[57], C.L. Da Silva[66], E. Dall'Occo[14], J. Dalseno[45], C. D'Ambrosio[47],
A. Danilina[38], P. d'Argent[47], A. Davis[61], O. De Aguiar Francisco[47], K. De Bruyn[47],
S. De Capua[61], M. De Cian[48], J.M. De Miranda[1], L. De Paula[2], M. De Serio[18,d], D. De Simone[49],
P. De Simone[22], J.A. de Vries[78], C.T. Dean[66], W. Dean[83], D. Decamp[8], L. Del Buono[12],
B. Delaney[54], H.-P. Dembinski[14], A. Dendek[34], V. Denysenko[49], D. Derkach[81], O. Deschamps[9],
F. Desse[11], F. Dettori[26,f], B. Dey[7], A. Di Canto[47], P. Di Nezza[22], S. Didenko[80],
L. Dieste Maronas[45], H. Dijkstra[47], V. Dobishuk[51], A.M. Donohoe[17], F. Dordei[26], M. Dorigo[28,y],
A.C. dos Reis[1], L. Douglas[58], A. Dovbnya[50], A.G. Downes[8], K. Dreimanis[59], M.W. Dudek[33],
L. Dufour[47], V. Duk[76], P. Durante[47], J.M. Durham[66], D. Dutta[61], M. Dziewiecki[16], A. Dziurda[33],
A. Dzyuba[37], S. Easo[56], U. Egede[69], V. Egorychev[38], S. Eidelman[42,x], S. Eisenhardt[57], S. Ek-In[48],
L. Eklund[58], S. Ely[67], A. Ene[36], E. Epple[66], S. Escher[13], J. Eschle[49], S. Esen[31], T. Evans[47],
A. Falabella[19], J. Fan[3], Y. Fan[5], B. Fang[72], N. Farley[52], S. Farry[59], D. Fazzini[11], P. Fedin[38],
M. Féo[47], P. Fernandez Declara[47], A. Fernandez Prieto[45], F. Ferrari[19,e], L. Ferreira Lopes[48],

F. Ferreira Rodrigues[2], S. Ferreres Sole[31], M. Ferrillo[49], M. Ferro-Luzzi[47], S. Filippov[40],
R.A. Fini[18], M. Fiorini[20,g], M. Firlej[34], K.M. Fischer[62], C. Fitzpatrick[61], T. Fiutowski[34],
F. Fleuret[11,b], M. Fontana[47], F. Fontanelli[23,i], R. Forty[47], V. Franco Lima[59], M. Franco Sevilla[65],
M. Frank[47], E. Franzoso[20], G. Frau[16], C. Frei[47], D.A. Friday[58], J. Fu[25,q], Q. Fuehring[14],
W. Funk[47], E. Gabriel[57], T. Gaintseva[41], A. Gallas Torreira[45], D. Galli[19,e], S. Gallorini[27],
S. Gambetta[57], Y. Gan[3], M. Gandelman[2], P. Gandini[25], Y. Gao[4], M. Garau[26],
L.M. Garcia Martin[46], P. Garcia Moreno[44], J. García Pardiñas[49], B. Garcia Plana[45],
F.A. Garcia Rosales[11], L. Garrido[44], D. Gascon[44], C. Gaspar[47], R.E. Geertsema[31], D. Gerick[16],
L.L. Gerken[14], E. Gersabeck[61], M. Gersabeck[61], T. Gershon[55], D. Gerstel[10], Ph. Ghez[8],
V. Gibson[54], M. Giovannetti[22,k], A. Gioventù[45], P. Gironella Gironell[44], L. Giubega[36],
C. Giugliano[20,g], K. Gizdov[57], E.L. Gkougkousis[47], V.V. Gligorov[12], C. Göbel[70],
E. Golobardes[44,m], D. Golubkov[38], A. Golutvin[60,80], A. Gomes[1,a], S. Gomez Fernandez[44],
M. Goncerz[33], G. Gong[3], P. Gorbounov[38], I.V. Gorelov[39], C. Gotti[24,j], E. Govorkova[31],
J.P. Grabowski[16], R. Graciani Diaz[44], T. Grammatico[12], L.A. Granado Cardoso[47], E. Graugés[44],
E. Graverini[48], G. Graziani[21], A. Grecu[36], L.M. Greeven[31], P. Griffith[20,g], L. Grillo[61],
S. Gromov[80], L. Gruber[47], B.R. Gruberg Cazon[62], C. Gu[3], M. Guarise[20], P. A. Günther[16],
E. Gushchin[40], A. Guth[13], Y. Guz[43,47], T. Gys[47], T. Hadavizadeh[62], G. Haefeli[48], C. Haen[47],
J. Haimberger[47], S.C. Haines[54], T. Halewood-leagas[59], P.M. Hamilton[65], Q. Han[7], X. Han[16],
T.H. Hancock[62], S. Hansmann-Menzemer[16], N. Harnew[62], T. Harrison[59], R. Hart[31], C. Hasse[47],
M. Hatch[47], J. He[5], M. Hecker[60], K. Heijhoff[31], K. Heinicke[14], A.M. Hennequin[47], K. Hennessy[59],
L. Henry[25,46], J. Heuel[13], A. Hicheur[68], D. Hill[62], M. Hilton[61], S.E. Hollitt[14], P.H. Hopchev[48],
J. Hu[16], J. Hu[71], W. Hu[7], W. Huang[5], X. Huang[72], W. Hulsbergen[31], T. Humair[60],
R.J. Hunter[55], M. Hushchyn[81], D. Hutchcroft[59], D. Hynds[31], P. Ibis[14], M. Idzik[34], D. Ilin[37],
P. Ilten[52], A. Inglessi[37], A. Ishteev[80], K. Ivshin[37], R. Jacobsson[47], S. Jakobsen[47], E. Jans[31],
B.K. Jashal[46], A. Jawahery[65], V. Jevtic[14], M. Jezabek[33], F. Jiang[3], M. John[62], D. Johnson[47],
C.R. Jones[54], T.P. Jones[55], B. Jost[47], N. Jurik[62], S. Kandybei[50], Y. Kang[3], M. Karacson[47],
J.M. Kariuki[53], N. Kazeev[81], M. Kecke[16], F. Keizer[54,47], M. Kelsey[67], M. Kenzie[55], T. Ketel[32],
B. Khanji[47], A. Kharisova[82], S. Kholodenko[43], K.E. Kim[67], T. Kirn[13], V.S. Kirsebom[48],
O. Kitouni[63], S. Klaver[22], K. Klimaszewski[35], S. Koliiev[51], A. Kondybayeva[80],
A. Konoplyannikov[38], P. Kopciewicz[34], R. Kopecna[16], P. Koppenburg[31], M. Korolev[39],
I. Kostiuk[31,51], O. Kot[51], S. Kotriakhova[37,30], P. Kravchenko[37], L. Kravchuk[40], R.D. Krawczyk[47],
M. Kreps[55], F. Kress[60], S. Kretzschmar[13], P. Krokovny[42,x], W. Krupa[34], W. Krzemien[35],
W. Kucewicz[33,l], M. Kucharczyk[33], V. Kudryavtsev[42,x], H.S. Kuindersma[31], G.J. Kunde[66],
T. Kvaratskheliya[38], D. Lacarrere[47], G. Lafferty[61], A. Lai[26], A. Lampis[26], D. Lancierini[49],
J.J. Lane[61], R. Lane[53], G. Lanfranchi[22], C. Langenbruch[13], J. Langer[14], O. Lantwin[49,80],
T. Latham[55], F. Lazzari[28,v], R. Le Gac[10], S.H. Lee[83], R. Lefèvre[9], A. Leflat[39,47], S. Legotin[80],
O. Leroy[10], T. Lesiak[33], B. Leverington[16], H. Li[71], L. Li[62], P. Li[16], X. Li[66], Y. Li[6], Y. Li[6], Z. Li[67],
X. Liang[67], T. Lin[60], R. Lindner[47], V. Lisovskyi[14], R. Litvinov[26], G. Liu[71], H. Liu[5], S. Liu[6],
X. Liu[3], A. Loi[26], J. Lomba Castro[45], I. Longstaff[58], J.H. Lopes[2], G. Loustau[49], G.H. Lovell[54],
Y. Lu[6], D. Lucchesi[27,o], S. Luchuk[40], M. Lucio Martinez[31], V. Lukashenko[31], Y. Luo[3],
A. Lupato[61], E. Luppi[20,g], O. Lupton[55], A. Lusiani[28,t], X. Lyu[5], L. Ma[6], S. Maccolini[19,e],
F. Machefert[11], F. Maciuc[36], V. Macko[48], P. Mackowiak[14], S. Maddrell-Mander[53],
L.R. Madhan Mohan[53], O. Maev[37], A. Maevskiy[81], D. Maisuzenko[37], M.W. Majewski[34],
S. Malde[62], B. Malecki[47], A. Malinin[79], T. Maltsev[42,x], H. Malygina[16], G. Manca[26,f],
G. Mancinelli[10], R. Manera Escalero[44], D. Manuzzi[19,e], D. Marangotto[25,q], J. Maratas[9,w],
J.F. Marchand[8], U. Marconi[19], S. Mariani[21,47,h], C. Marin Benito[11], M. Marinangeli[48],
P. Marino[48], J. Marks[16], P.J. Marshall[59], G. Martellotti[30], L. Martinazzoli[47], M. Martinelli[24,j],
D. Martinez Santos[45], F. Martinez Vidal[46], A. Massafferri[1], M. Materok[13], R. Matev[47],

A. Mathad[49], Z. Mathe[47], V. Matiunin[38], C. Matteuzzi[24], K.R. Mattioli[83], A. Mauri[49],
E. Maurice[11,b], J. Mauricio[44], M. Mazurek[35], M. McCann[60], L. Mcconnell[17], T.H. Mcgrath[61],
A. McNab[61], R. McNulty[17], J.V. Mead[59], B. Meadows[64], C. Meaux[10], G. Meier[14], N. Meinert[75],
D. Melnychuk[35], S. Meloni[24,j], M. Merk[31], A. Merli[25], L. Meyer Garcia[2], M. Mikhasenko[47],
D.A. Milanes[73], E. Millard[55], M.-N. Minard[8], O. Mineev[38], L. Minzoni[20,g], S.E. Mitchell[57],
B. Mitreska[61], D.S. Mitzel[47], A. Mödden[14], A. Mogini[12], R.A. Mohammed[62], R.D. Moise[60],
T. Mombächer[14], I.A. Monroy[73], S. Monteil[9], M. Morandin[27], G. Morello[22], M.J. Morello[28,t],
J. Moron[34], A.B. Morris[74], A.G. Morris[55], R. Mountain[67], H. Mu[3], F. Muheim[57], M. Mukherjee[7],
M. Mulder[47], D. Müller[47], K. Müller[49], C.H. Murphy[62], D. Murray[61], P. Muzzetto[26], P. Naik[53],
T. Nakada[48], R. Nandakumar[56], T. Nanut[48], I. Nasteva[2], M. Needham[57], I. Neri[20,g], N. Neri[25,q],
S. Neubert[16], N. Neufeld[47], R. Newcombe[60], T.D. Nguyen[48], C. Nguyen-Mau[48,n], E.M. Niel[11],
S. Nieswand[13], N. Nikitin[39], N.S. Nolte[47], C. Nunez[83], A. Oblakowska-Mucha[34], V. Obraztsov[43],
S. Ogilvy[58], D.P. O'Hanlon[53], R. Oldeman[26,f], C.J.G. Onderwater[77], J. D. Osborn[83],
A. Ossowska[33], J.M. Otalora Goicochea[2], T. Ovsiannikova[38], P. Owen[49], A. Oyanguren[46],
B. Pagare[55], P.R. Pais[47], T. Pajero[28,47,t], A. Palano[18], M. Palutan[22], Y. Pan[61], G. Panshin[82],
A. Papanestis[56], M. Pappagallo[57], L.L. Pappalardo[20,g], C. Pappenheimer[64], W. Parker[65],
C. Parkes[61], C.J. Parkinson[45], B. Passalacqua[20], G. Passaleva[21,47], A. Pastore[18], M. Patel[60],
C. Patrignani[19,e], C.J. Pawley[78], A. Pearce[47], A. Pellegrino[31], M. Pepe Altarelli[47], S. Perazzini[19],
D. Pereima[38], P. Perret[9], K. Petridis[53], A. Petrolini[23,i], A. Petrov[79], S. Petrucci[57],
M. Petruzzo[25,q], A. Philippov[41], L. Pica[28], M. Piccini[76], B. Pietrzyk[8], G. Pietrzyk[48], M. Pili[62],
D. Pinci[30], J. Pinzino[47], F. Pisani[19], A. Piucci[16], Resmi P.K[10], V. Placinta[36], S. Playfer[57],
J. Plews[52], M. Plo Casasus[45], F. Polci[12], M. Poli Lener[22], M. Poliakova[67], A. Poluektov[10],
N. Polukhina[80,c], I. Polyakov[67], E. Polycarpo[2], G.J. Pomery[53], S. Ponce[47], A. Popov[43],
D. Popov[52], S. Popov[41], S. Poslavskii[43], K. Prasanth[33], L. Promberger[47], C. Prouve[45],
V. Pugatch[51], A. Puig Navarro[49], H. Pullen[62], G. Punzi[28,p], W. Qian[5], J. Qin[5], R. Quagliani[12],
B. Quintana[8], N.V. Raab[17], R.I. Rabadan Trejo[10], B. Rachwal[34], J.H. Rademacker[53], M. Rama[28],
M. Ramos Pernas[45], M.S. Rangel[2], F. Ratnikov[41,81], G. Raven[32], M. Reboud[8], F. Redi[48],
F. Reiss[12], C. Remon Alepuz[46], Z. Ren[3], V. Renaudin[62], R. Ribatti[28], S. Ricciardi[56],
D.S. Richards[56], S. Richards[53], K. Rinnert[59], P. Robbe[11], A. Robert[12], G. Robertson[57],
A.B. Rodrigues[48], E. Rodrigues[59], J.A. Rodriguez Lopez[73], M. Roehrken[47], A. Rollings[62],
P. Roloff[47], V. Romanovskiy[43], M. Romero Lamas[45], A. Romero Vidal[45], J.D. Roth[83],
M. Rotondo[22], M.S. Rudolph[67], T. Ruf[47], J. Ruiz Vidal[46], A. Ryzhikov[81], J. Ryzka[34],
J.J. Saborido Silva[45], N. Sagidova[37], N. Sahoo[55], B. Saitta[26,f], C. Sanchez Gras[31],
C. Sanchez Mayordomo[46], R. Santacesaria[30], C. Santamarina Rios[45], M. Santimaria[22],
E. Santovetti[29,k], D. Saranin[80], G. Sarpis[61], M. Sarpis[16], A. Sarti[30], C. Satriano[30,s], A. Satta[29],
M. Saur[5], D. Savrina[38,39], H. Sazak[9], L.G. Scantlebury Smead[62], S. Schael[13], M. Schellenberg[14],
M. Schiller[58], H. Schindler[47], M. Schmelling[15], T. Schmelzer[14], B. Schmidt[47], O. Schneider[48],
A. Schopper[47], H.F. Schreiner[64], M. Schubiger[31], S. Schulte[48], M.H. Schune[11], R. Schwemmer[47],
B. Sciascia[22], A. Sciubba[30], S. Sellam[68], A. Semennikov[38], M. Senghi Soares[32], A. Sergi[52,47],
N. Serra[49], J. Serrano[10], L. Sestini[27], A. Seuthe[14], P. Seyfert[47], D.M. Shangase[83], M. Shapkin[43],
I. Shchemerov[80], L. Shchutska[48], T. Shears[59], L. Shekhtman[42,x], Z. Shen[4], V. Shevchenko[79],
E.B. Shields[24,j], E. Shmanin[80], J.D. Shupperd[67], B.G. Siddi[20], R. Silva Coutinho[49],
L. Silva de Oliveira[2], G. Simi[27,o], S. Simone[18,d], I. Skiba[20,g], N. Skidmore[16], T. Skwarnicki[67],
M.W. Slater[52], J.C. Smallwood[62], J.G. Smeaton[54], A. Smetkina[38], E. Smith[13], I.T. Smith[57],
M. Smith[60], A. Snoch[31], M. Soares[19], L. Soares Lavra[9], M.D. Sokoloff[64], F.J.P. Soler[58],
A. Solovev[37], I. Solovyev[37], F.L. Souza De Almeida[2], B. Souza De Paula[2], B. Spaan[14],
E. Spadaro Norella[25,q], P. Spradlin[58], F. Stagni[47], M. Stahl[64], S. Stahl[47], P. Stefko[48],
O. Steinkamp[49,80], S. Stemmle[16], O. Stenyakin[43], M. Stepanova[37], H. Stevens[14], S. Stone[67],

M.E. Stramaglia[48], M. Straticiuc[36], D. Strekalina[80], S. Strokov[82], F. Suljik[62], J. Sun[26], L. Sun[72],
Y. Sun[65], P. Svihra[61], P.N. Swallow[52], K. Swientek[34], A. Szabelski[35], T. Szumlak[34],
M. Szymanski[47], S. Taneja[61], Z. Tang[3], T. Tekampe[14], F. Teubert[47], E. Thomas[47],
K.A. Thomson[59], M.J. Tilley[60], V. Tisserand[9], S. T'Jampens[8], M. Tobin[6], S. Tolk[47],
L. Tomassetti[20,g], D. Torres Machado[1], D.Y. Tou[12], E. Tournefier[8], M. Traill[58], M.T. Tran[48],
E. Trifonova[80], C. Trippl[48], A. Tsaregorodtsev[10], G. Tuci[28,p], A. Tully[48], N. Tuning[31],
A. Ukleja[35], D.J. Unverzagt[16], A. Usachov[31], A. Ustyuzhanin[41,81], U. Uwer[16], A. Vagner[82],
V. Vagnoni[19], A. Valassi[47], G. Valenti[19], N. Valls Canudas[44], M. van Beuzekom[31],
H. Van Hecke[66], E. van Herwijnen[80], C.B. Van Hulse[17], M. van Veghel[77], R. Vazquez Gomez[44],
P. Vazquez Regueiro[45], C. Vázquez Sierra[31], S. Vecchi[20], J.J. Velthuis[53], M. Veltri[21,r],
A. Venkateswaran[67], M. Veronesi[31], M. Vesterinen[55], J.V. Viana Barbosa[47], D. Vieira[64],
M. Vieites Diaz[48], H. Viemann[75], X. Vilasis-Cardona[44], E. Vilella Figueras[59], P. Vincent[12],
G. Vitali[28], A. Vitkovskiy[31], A. Vollhardt[49], D. Vom Bruch[12], A. Vorobyev[37], V. Vorobyev[42,x],
N. Voropaev[37], R. Waldi[75], J. Walsh[28], C. Wang[16], J. Wang[3], J. Wang[72], J. Wang[4], J. Wang[6],
M. Wang[3], R. Wang[53], Y. Wang[7], Z. Wang[49], D.R. Ward[54], H.M. Wark[59], N.K. Watson[52],
S.G. Weber[12], D. Websdale[60], A. Weiden[49], C. Weisser[63], B.D.C. Westhenry[53], D.J. White[61],
M. Whitehead[53], D. Wiedner[14], G. Wilkinson[62], M. Wilkinson[67], I. Williams[54], M. Williams[63,69],
M.R.J. Williams[61], T. Williams[52], F.F. Wilson[56], W. Wislicki[35], M. Witek[33], L. Witola[16],
G. Wormser[11], S.A. Wotton[54], H. Wu[67], K. Wyllie[47], Z. Xiang[5], D. Xiao[7], Y. Xie[7], H. Xing[71],
A. Xu[4], J. Xu[5], L. Xu[3], M. Xu[7], Q. Xu[5], Z. Xu[5], Z. Xu[4], D. Yang[3], Y. Yang[5], Z. Yang[3],
Z. Yang[65], Y. Yao[67], L.E. Yeomans[59], H. Yin[7], J. Yu[7], X. Yuan[67], O. Yushchenko[43],
K.A. Zarebski[52], M. Zavertyaev[15,c], M. Zdybal[33], O. Zenaiev[47], M. Zeng[3], D. Zhang[7], L. Zhang[3],
S. Zhang[4], Y. Zhang[47], A. Zhelezov[16], Y. Zheng[5], X. Zhou[5], Y. Zhou[5], X. Zhu[3], V. Zhukov[13,39],
J.B. Zonneveld[57], S. Zucchelli[19,e], D. Zuliani[27], G. Zunica[61]

1   Centro Brasileiro de Pesquisas Físicas (CBPF), Rio de Janeiro, Brazil
2   Universidade Federal do Rio de Janeiro (UFRJ), Rio de Janeiro, Brazil
3   Center for High Energy Physics, Tsinghua University, Beijing, China
4   School of Physics State Key Laboratory of Nuclear Physics and Technology, Peking University,
    Beijing, China
5   University of Chinese Academy of Sciences, Beijing, China
6   Institute Of High Energy Physics (IHEP), Beijing, China
7   Institute of Particle Physics, Central China Normal University, Wuhan, Hubei, China
8   Univ. Grenoble Alpes, Univ. Savoie Mont Blanc, CNRS, IN2P3-LAPP, Annecy, France
9   Université Clermont Auvergne, CNRS/IN2P3, LPC, Clermont-Ferrand, France
10 Aix Marseille Univ, CNRS/IN2P3, CPPM, Marseille, France
11 Université Paris-Saclay, CNRS/IN2P3, IJCLab, Orsay, France
12 LPNHE, Sorbonne Université, Paris Diderot Sorbonne Paris Cité, CNRS/IN2P3, Paris, France
13 I. Physikalisches Institut, RWTH Aachen University, Aachen, Germany
14 Fakultät Physik, Technische Universität Dortmund, Dortmund, Germany
15 Max-Planck-Institut für Kernphysik (MPIK), Heidelberg, Germany
16 Physikalisches Institut, Ruprecht-Karls-Universität Heidelberg, Heidelberg, Germany
17 School of Physics, University College Dublin, Dublin, Ireland
18 INFN Sezione di Bari, Bari, Italy
19 INFN Sezione di Bologna, Bologna, Italy
20 INFN Sezione di Ferrara, Ferrara, Italy
21 INFN Sezione di Firenze, Firenze, Italy
22 INFN Laboratori Nazionali di Frascati, Frascati, Italy
23 INFN Sezione di Genova, Genova, Italy
24 INFN Sezione di Milano-Bicocca, Milano, Italy

25 *INFN Sezione di Milano, Milano, Italy*

26 *INFN Sezione di Cagliari, Monserrato, Italy*

27 *Universita degli Studi di Padova, Universita e INFN, Padova, Padova, Italy*

28 *INFN Sezione di Pisa, Pisa, Italy*

29 *INFN Sezione di Roma Tor Vergata, Roma, Italy*

30 *INFN Sezione di Roma La Sapienza, Roma, Italy*

31 *Nikhef National Institute for Subatomic Physics, Amsterdam, Netherlands*

32 *Nikhef National Institute for Subatomic Physics and VU University Amsterdam, Amsterdam, Netherlands*

33 *Henryk Niewodniczanski Institute of Nuclear Physics Polish Academy of Sciences, Kraków, Poland*

34 *AGH - University of Science and Technology, Faculty of Physics and Applied Computer Science, Kraków, Poland*

35 *National Center for Nuclear Research (NCBJ), Warsaw, Poland*

36 *Horia Hulubei National Institute of Physics and Nuclear Engineering, Bucharest-Magurele, Romania*

37 *Petersburg Nuclear Physics Institute NRC Kurchatov Institute (PNPI NRC KI), Gatchina, Russia*

38 *Institute of Theoretical and Experimental Physics NRC Kurchatov Institute (ITEP NRC KI), Moscow, Russia, Moscow, Russia*

39 *Institute of Nuclear Physics, Moscow State University (SINP MSU), Moscow, Russia*

40 *Institute for Nuclear Research of the Russian Academy of Sciences (INR RAS), Moscow, Russia*

41 *Yandex School of Data Analysis, Moscow, Russia*

42 *Budker Institute of Nuclear Physics (SB RAS), Novosibirsk, Russia*

43 *Institute for High Energy Physics NRC Kurchatov Institute (IHEP NRC KI), Protvino, Russia, Protvino, Russia*

44 *ICCUB, Universitat de Barcelona, Barcelona, Spain*

45 *Instituto Galego de Física de Altas Enerxías (IGFAE), Universidade de Santiago de Compostela, Santiago de Compostela, Spain*

46 *Instituto de Fisica Corpuscular, Centro Mixto Universidad de Valencia - CSIC, Valencia, Spain*

47 *European Organization for Nuclear Research (CERN), Geneva, Switzerland*

48 *Institute of Physics, Ecole Polytechnique Fédérale de Lausanne (EPFL), Lausanne, Switzerland*

49 *Physik-Institut, Universität Zürich, Zürich, Switzerland*

50 *NSC Kharkiv Institute of Physics and Technology (NSC KIPT), Kharkiv, Ukraine*

51 *Institute for Nuclear Research of the National Academy of Sciences (KINR), Kyiv, Ukraine*

52 *University of Birmingham, Birmingham, United Kingdom*

53 *H.H. Wills Physics Laboratory, University of Bristol, Bristol, United Kingdom*

54 *Cavendish Laboratory, University of Cambridge, Cambridge, United Kingdom*

55 *Department of Physics, University of Warwick, Coventry, United Kingdom*

56 *STFC Rutherford Appleton Laboratory, Didcot, United Kingdom*

57 *School of Physics and Astronomy, University of Edinburgh, Edinburgh, United Kingdom*

58 *School of Physics and Astronomy, University of Glasgow, Glasgow, United Kingdom*

59 *Oliver Lodge Laboratory, University of Liverpool, Liverpool, United Kingdom*

60 *Imperial College London, London, United Kingdom*

61 *Department of Physics and Astronomy, University of Manchester, Manchester, United Kingdom*

62 *Department of Physics, University of Oxford, Oxford, United Kingdom*

63 *Massachusetts Institute of Technology, Cambridge, MA, United States*

64 *University of Cincinnati, Cincinnati, OH, United States*

65 *University of Maryland, College Park, MD, United States*

66 *Los Alamos National Laboratory (LANL), Los Alamos, United States*

67 *Syracuse University, Syracuse, NY, United States*

68 *Laboratory of Mathematical and Subatomic Physics , Constantine, Algeria, associated to [2]*

69 *School of Physics and Astronomy, Monash University, Melbourne, Australia, associated to [55]*

[70] Pontifícia Universidade Católica do Rio de Janeiro (PUC-Rio), Rio de Janeiro, Brazil, associated to [2]

[71] Guangdong Provencial Key Laboratory of Nuclear Science, Institute of Quantum Matter, South China Normal University, Guangzhou, China, associated to [3]

[72] School of Physics and Technology, Wuhan University, Wuhan, China, associated to [3]

[73] Departamento de Fisica , Universidad Nacional de Colombia, Bogota, Colombia, associated to [12]

[74] Universität Bonn - Helmholtz-Institut für Strahlen und Kernphysik, Bonn, Germany, associated to [16]

[75] Institut für Physik, Universität Rostock, Rostock, Germany, associated to [16]

[76] INFN Sezione di Perugia, Perugia, Italy, associated to [20]

[77] Van Swinderen Institute, University of Groningen, Groningen, Netherlands, associated to [31]

[78] Universiteit Maastricht, Maastricht, Netherlands, associated to [31]

[79] National Research Centre Kurchatov Institute, Moscow, Russia, associated to [38]

[80] National University of Science and Technology "MISIS", Moscow, Russia, associated to [38]

[81] National Research University Higher School of Economics, Moscow, Russia, associated to [41]

[82] National Research Tomsk Polytechnic University, Tomsk, Russia, associated to [38]

[83] University of Michigan, Ann Arbor, United States, associated to [67]

[a] Universidade Federal do Triângulo Mineiro (UFTM), Uberaba-MG, Brazil

[b] Laboratoire Leprince-Ringuet, Palaiseau, France

[c] P.N. Lebedev Physical Institute, Russian Academy of Science (LPI RAS), Moscow, Russia

[d] Università di Bari, Bari, Italy

[e] Università di Bologna, Bologna, Italy

[f] Università di Cagliari, Cagliari, Italy

[g] Università di Ferrara, Ferrara, Italy

[h] Università di Firenze, Firenze, Italy

[i] Università di Genova, Genova, Italy

[j] Università di Milano Bicocca, Milano, Italy

[k] Università di Roma Tor Vergata, Roma, Italy

[l] AGH - University of Science and Technology, Faculty of Computer Science, Electronics and Telecommunications, Kraków, Poland

[m] DS4DS, La Salle, Universitat Ramon Llull, Barcelona, Spain

[n] Hanoi University of Science, Hanoi, Vietnam

[o] Università di Padova, Padova, Italy

[p] Università di Pisa, Pisa, Italy

[q] Università degli Studi di Milano, Milano, Italy

[r] Università di Urbino, Urbino, Italy

[s] Università della Basilicata, Potenza, Italy

[t] Scuola Normale Superiore, Pisa, Italy

[u] Università di Modena e Reggio Emilia, Modena, Italy

[v] Università di Siena, Siena, Italy

[w] MSU - Iligan Institute of Technology (MSU-IIT), Iligan, Philippines

[x] Novosibirsk State University, Novosibirsk, Russia

[y] INFN Sezione di Trieste, Trieste, Italy

[z] Universidad Nacional Autonoma de Honduras, Tegucigalpa, Honduras